Egypt. J. Chem. **Vol. 65**, No. 11 pp. 691- 705 (2022)

Egyptian Journal of Chemistry

http://ejchem.journals.ekb.eg/

Synthesis of new Corrosion Inhibitor from Nano-Polymer and study its adsorption on carbon steel at different Temperatures

Doaa. R. Mohammedali[*1], Hamida. I. Salman[1], Mohammed. N. Bahjat[1], Emad Salaam Abood[2]

[1]*Chemistry Department, College of Education for Pure Sciences, University of Kerbala, Kerbala, Iraq*

[2]*Medical physics department, Hilla University College, Babylon, Iraq*

Abstract

In this research, the nanoparticle graft co-polymer was prepared, by reacting glycerol with terphthalic acid as a first step, and in the second step added maleic anhydride to prepare graft co-polymer by solubilization process. Fixed weights of the Poly (Terphthalic acid-co-Glycerol-G-Maleic anhydride) were mixed with different weights of acrylic acid (0.2 – 0.4 – 0.6 –and 0.8 mol) with the addition of drops of cobalt octoate to get different concentrations of the inhibitor. Carbon steel ingots were coated with these concentrations and the inhibition efficiency was calculated at different temperatures (303 –313 –323) k with a fixed time of 30 minutes. The highest results of inhibition efficiency recorded 91.41% at concentration 0.8 mol of Nano-polymer and at 303 K .

Keywords: Corrosion; Carbon Steel; Nano-Polymer, Inhibitor; Coating; Co-polymer

1. Introduction

Nanotechnology has wide applications in research. Nanoparticles have size ranges from 1 to 100 nm and They have used in different areas like industrial[1, 2], environmental [3], biomedical [4], agriculture [5] and food [6-9]. They have unique and superior elementary physical and chemical properties for example higher outward area, mechanical strength, optical active and chemical reactive [10, 11]. From the most important uses for nanoparticles in industrial field is having a great ability to protect the metal from corrosion in different environments [12, 13]. Corrosion occurs when metals interact with their surroundings. The metal converts into a more chemically stable form such as oxide, hydroxide, or sulfide by the chemical or electrochemical reactions metal and environment. Corrosion is the biggest problem of the world because it damage or destruction of material. The cost of the corrosion is equal to about 4% of the gross national product [14-16]. There are many different ways are used to reduce corrosion rate such as metal surface coating, using corrosion inhibitors, Environmental Modifications, change in pH and potential by cathodic or anodic reaction[17]. The most common methods to decrease the corrosion rate are using inhibitors. These inhibitors reduce the corrosion rate by forming protective film on the metal surface. There are many organic and inorganic inhibitors used to reduce corrosion especially the organic compounds that have heteroatoms in their structures (such as N , O , S), aromatic ring, certain functional groups , and conjugated varied bonds ,These factors enable organic inhibitors to adsorb on metals surfaces and decrease corrosion[18-20]. But these inhibitors don't prefer because they are very expensive and toxic for environment. So these inhibitors are replaced by nanomaterials inhibitors. Nano compounds are blocking active sites of metal surface so it can reduce the rate of corrosion and also provide hardness, straight, durability, optical qualities and thermal stability[21]. So the aim of this article forming new inhibitor (Nano-Polymer) which has high molecular weight, environmentally friendly, less expensive, more effective, and safe to minimize corrosion. The mechanism of inhibition (of the polymer used) can be explained that its adsorption increases on the metal surface through the electrons of the pi bonds of the aromatic rings and the free (unlinked) electron pairs of oxygen in

*Corresponding author e-mail: doaa.r@s.uokerbala.edu.iq; (Doaa. R. Mohammedali).

Receive Date: 17 May 2022; Revise Date: 25 May 2022; Accept Date: 31 May 2022.

DOI: 10.21608/EJCHEM.2022.139171.6113.

the hydroxyl (OH) and carbonyl (CO) groups. Since the oxygen atoms in the polymer will give a pair of unbonded electron to the empty orbital in the metal, thus strong stable bonds will be formed between the metal surface and the inhibitor (polymer).[22]

2. Experimental

All chemicals were supplied by chemical companies. The electrochemical measurements were performed on MLab 200 Potentiostat / Galvanostat.

2.1. Synthesis of Poly Terphthalic acid-co-Glycerol-G-Maleic anhydride graft (PTGM) Nano-particles (5):

It was synthesized by two steps

The first step: formed Linear Nano co-polymer (3)

A mixture of compound terephthalic acid **(1)** (2.0 mole, 332g) and (50 ml) dimethylsulphoxide (DMSO) was warmed to 40^{o}C in two-necked round bottom flask. This flask was equipped with a thermometer until clear liquor is formed. Adding (1.0 mole, 92gm) from glycerol (2) and heating the mixture to 120 ^{o}C. p-Xylene (25 ml) was added in two stages carefully to withdraw the water resulting from the esterification process. The flask was gently heated at 145^{o}C for 80 min. The reaction was cooled to 50 ^{o}C to give Linear Nano co-polymer **3**

Linear Nano co-polymer (3), yield 95%; IR (KBr):~ν = 3423 (br, OH alcoholic), 2902 (OH carboxylic acid), 2654, 2544, (C-H sp^{3}and sp^{2} hybridization absorption), 1726 (C═O ester group), 1597, 1581 (C=C), 1284 -1259 (C-O) cm $^{-1}$; ^{1}H NMR (500 MHz, $CDCl_3$): δ = 13.24 (s, 2H, COOH),7.53- 8.10 (m, 8H, CH- aromatics), 6.27-6.46 (d, 4H, methylene), 4.24- 4.50 (m, 1H, methyl), 3.44- 3.62 (t, 1H, aliphatic alcohol;) ppm (Fig. 1 and 2).

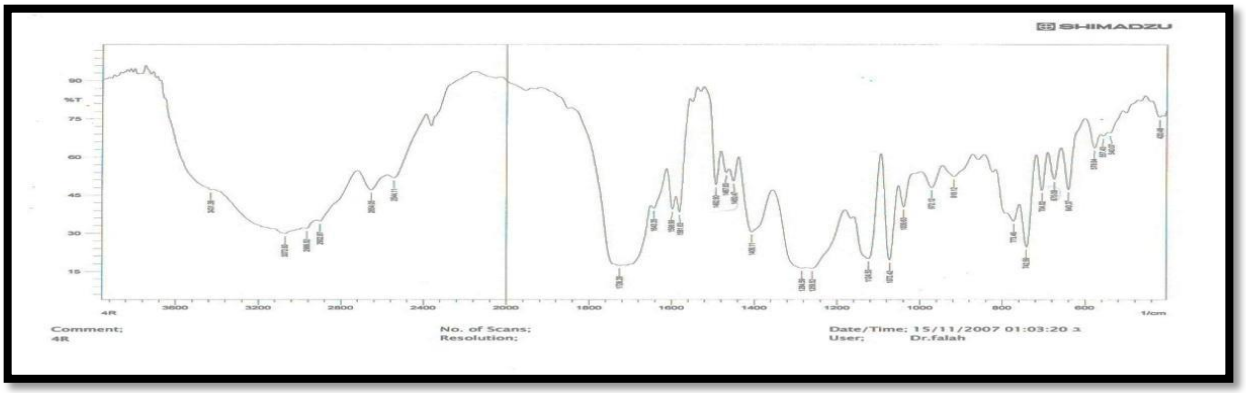

Figure (1): The FT-IR spectrum of linear co-polymer

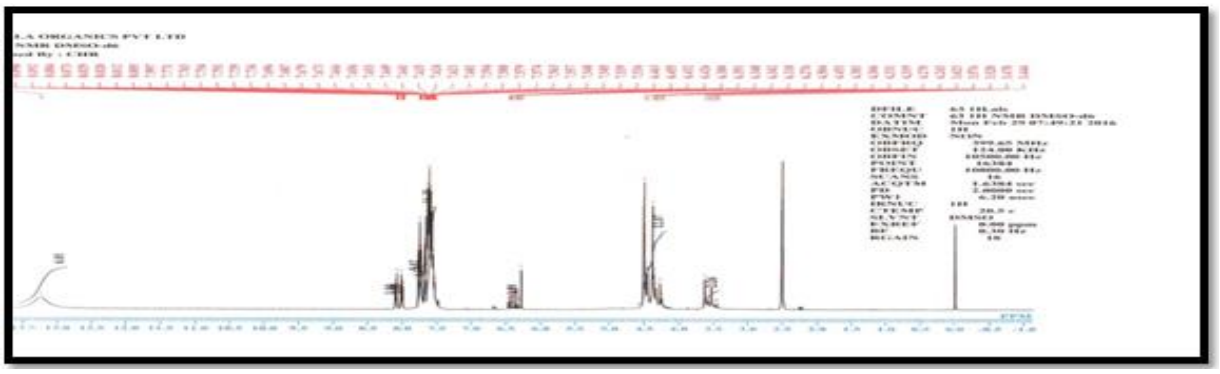

Figure (2): The ^{1}HNMR spectrum of linear co-polymer

The second step;

Dissolving (0.5 mol, 58 g) of maleic anhydride **(4**) in 10 ml DMSO at 40^{o}C then added to Linear Nano co-polymer **3.** The mixture was gently heated to 90^{o}C, the drops of p-xylene was added in two stages carefully to withdraw the water at 105^{o}C. After 40 min. the reaction mixture was cooled to room temperature. Leave the reaction mixture at room temperature for 6h. Adding the cold distilled water to the reaction to form the suspension solution and leave overnight. The ppt was filtered and washed with distilled water to form PTGM Nano Particals **.**

5.Poly Terphthalic acid-co-Glycerol-G-Maleic anhydride graft (PTGM) Nano-particles (5):

IR (KBr):~ν = 3500 for stretching alcoholic -OH with stretching (H–bond), 3140 aromatic =C-H, 3050 alkenes =C–H, 2880 aliphatic C-H, 1740 C=O ester and 1250 C-O ester cm^{-1}. The spectrum of ^{1}HNMR (600 MHz, $(CD_3)_3SO$) δ = 13.12 (s, Protons of carboxylic groups), 7.79-7.48 (m, protons of aromatic ring), 6.46 (d, CH of maleic anhydride), 5.91-5.56 (d, C$\underline{H_2}$-CH-CH_2), 4.28-4.23 (m, CH_2-C$\underline{H}$-CH_2). (Fig. 3, 4)

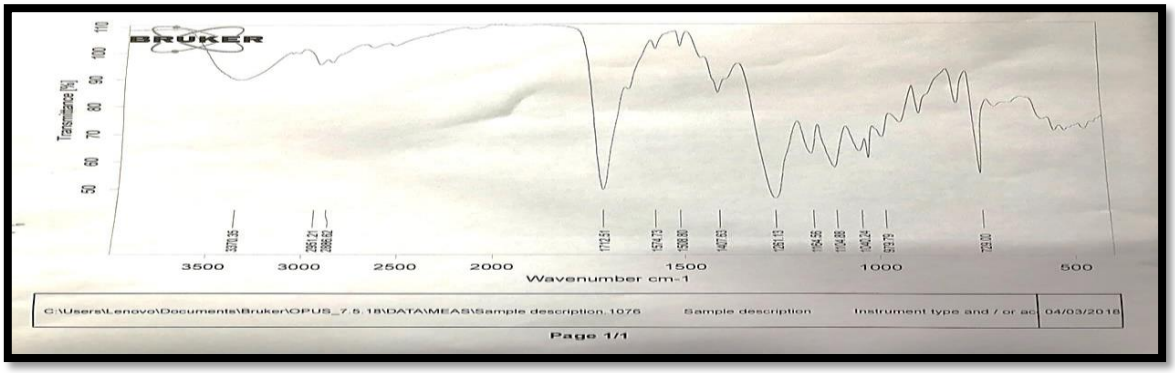

Figure (3): The FT-IR spectrum of graft co-polymer

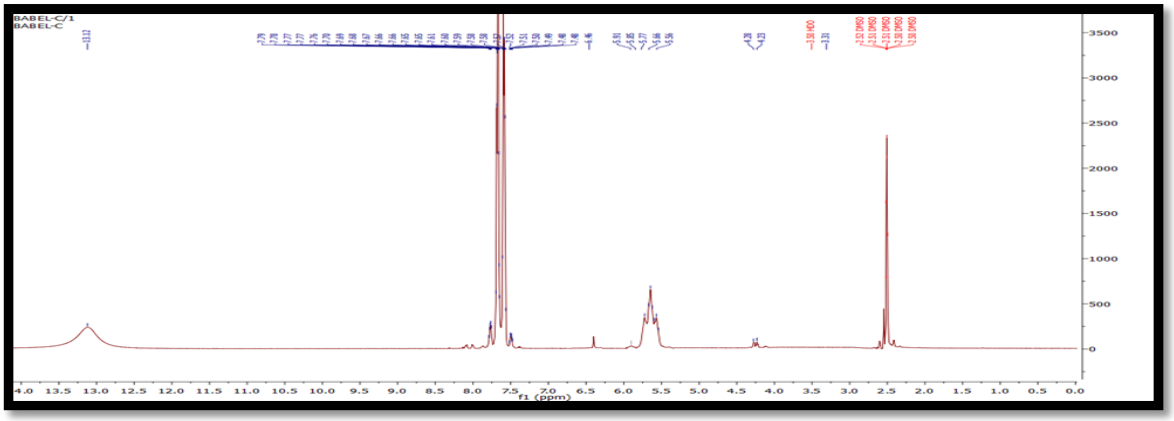

Figure (4): The ^{1}HNMR spectrum of graft co-polyme

2.2. Preparation of carbon steel specimens:

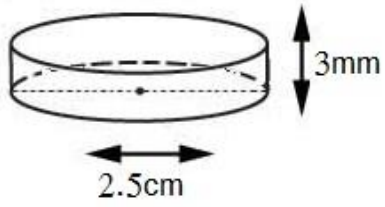

Figure (5): schematic diagram of carbon steel specimen

Cylindrical shaped carbon steel specimens (2.5 cm diameter and 3 mm height), as illustrated in Figure (5), with chemical composition 0.462% C, 0.260% Si, 0.597% Mn,0.0108% P, 0.0215% S, 0.0877% Cr, 0.0206% Mo, 0.0974% Ni, 0.0275% Al, 0.297% Cu and Fe balanced.. The specimens were grounded with emery paper of fine grain size (grade 80–400), Then the specimens were washed, dried and stored until use.

2.3. Preparation of coating:

A mixture of (0.1 g , 1.168 * 10^{-4} mol) nano-polymer with different mols (0.2, 0.4, 0.6, 0.8 mol) of acrylic acid, and add (2-3) drops of (cobalt octoate and hardener) with continuous mixing, until forming the orange solution. Coating carbon steel specimens with this solution, and dry it. Figure (6)

2.4. Preparation of Corrosive environment solutions:

The attacker solution 1M H_2SO_4 was prepared through mitigation of analytical degree 98% H_2SO_4 solution with distilled water.

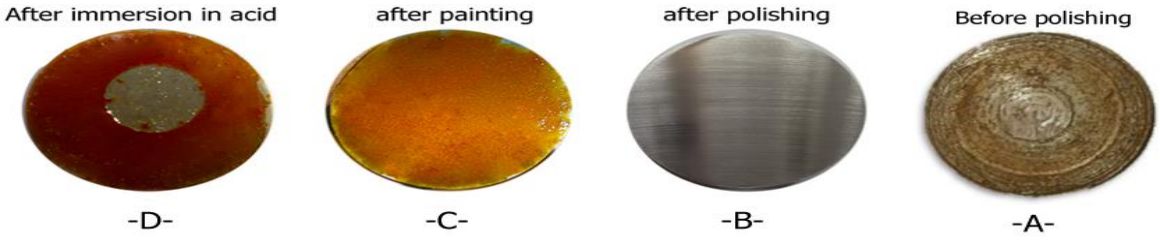

Figure (6): shape of carbon steel specimens

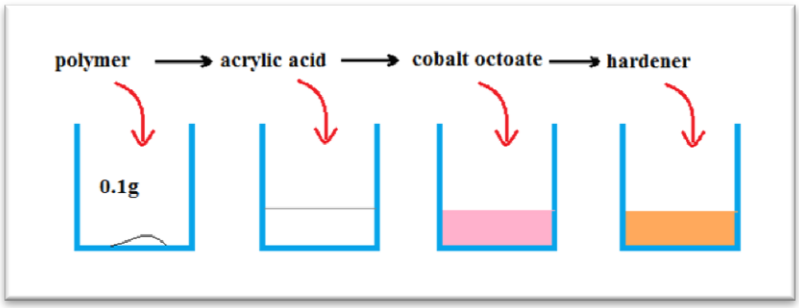

Figure (7): Preparation of coating

2.5. Potentiostatic Polarization Measurements:

Potentiostatic polarization measurements were conducted in a cell consists of three electrodes, reference electrode (calomel electrode RE), auxiliary electrode (platinum electrode AE), and working electrode (carbon steel specimens WE). The working electrode was dipped into the test solution for 30 min, with a time step of 1 sec and left to attain steady-state open circuit potential (OCP). Potential range was auto (±250 mv) relative to the OCP. The corrosion potential (E_{corr}) and corrosion current density (I_{corr}) were measured by tafel method. The inhibition efficiency (Ƞ%) was calculated as in equation (1) [23].

$$\eta\% = \frac{I_{corr} - I_{inh}}{I_{corr}} \times 100\ \% \quad \text{..... equation (1)}$$

Where Ƞ% is the ratio of the efficiency of inhibition. I_{corr} , I_{inh} is corrosion current density in the absence and presence of inhibitors

3. Results and Discussion

Terephthalic acid **(1)** reacted with glycerol (**2**) to form ester (**3)**. The most characteristic features of Linear nano co-polymer **3** are IR spectrum (fig 1) showed the appearance of a strong broad band at about 3423 cm^{-1} for stretching alcoholic -OH with stretching (H–bond), and at 1726 cm^{-1} strong band C=O ester group.[24] The spectrum of ^{1}HNMR showed the presence of singlet signal at 13.24 ppm characteristic of proton in carboxylic acid group, the signals at 6.27-6.46 ppm for four protons of methylene in the structure of co-polymer, the multiples at 4.24- 4.50 ppm of methyl protons, and the triplet signal in 3.44- 3.62 ppm due to the proton of aliphatic alcohol so this spectrum was confirmed the structure of our target polymer [25, 26]. (Scheme 1)

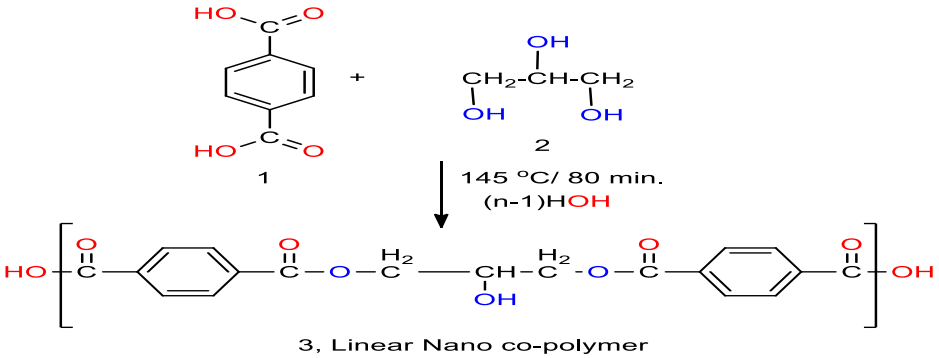

Scheme 1

As shown in (Scheme 2) ester **3** was reacted with maleic anhydride **(4)** to give Poly Terphthalic acid-co-Glycerol-G-Maleic anhydride graft (PTGM) Nano-particles (**5**). The structural assignment of compounds **5** was based upon spectroscopic data for example IR showed the appearance of a strong broad band at 3500 cm^{-1} for stretching alcoholic -OH with stretching (H–bond), and the spectrum also showed a strong sharp band at 1740 cm^{-1} and 1250 cm^{-1} for a stretching band C=O ester and C-O ester respectively. The spectrum of ^{1}HNMR (600 MHz, $(CD_3)_3SO$) showed the appearance 13.12 (s, COOH), 6.46 (d, CH of maleic anhydride), 5.91-5.56 (d, C$\underline{H_2}$-CH-CH_2), 4.28-4.23 (m, CH_2-C$\underline{H}$-CH_2).

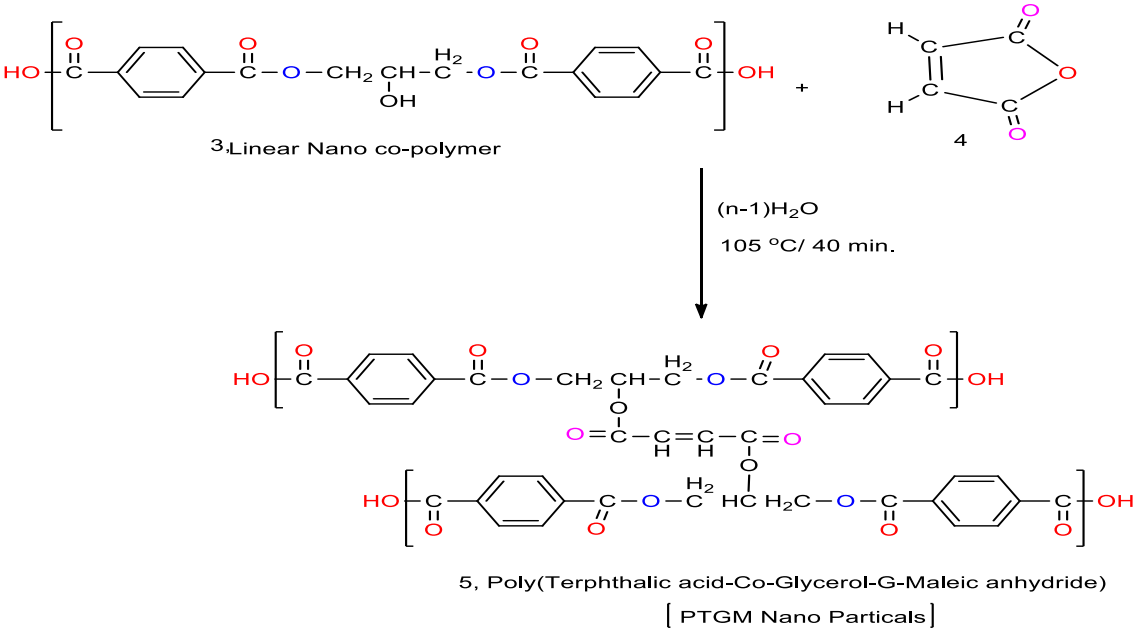

Scheme 2

By using solubilization process we prepared the linear and graft co-polymers in the size of nano particles, which measured by atomic force microscope (AFM), fig (8a-c) shows the outer surface of the nanoparticles of linear co-polymer. The roughness of this surface and the square root square are calculated according to the coefficient:

$$Rm \sqrt{\sum_{i=1}^{n} \frac{(Zi - Zav)^2}{N}}$$

Where N, Z = the number of measured points

The bold size of the nanoparticles has an important role in the roughness of the surface, surface homogeneity, and its uniform crystalline system. As shown in (Fig. 8a-c), the roughness coefficient of a linear co-polymer surface was 1.19 nm, the square root square was equal to 1.37 nm and the average of height of the particles was equal to 4.80 nm. (Fig. 9) is shown the distribution of the different proportions of particle sizes of the linear co-polymer nanoparticle. Table (1), represents the total rate of the particle sizes of the common linear nanoparticle and the different proportions of these volumes; the results indicate that the molecular size of the linear co-polymer nanoparticle was 94.09 nm. On the other hand, (Fig. 10a-c) represents the outer surface of the nanoparticles of graft co-polymer. The roughness coefficient of a graft co-polymer surface was 2.12 nm, the square root square was equal to 2.44 nm and the average of height of the particles was equal to 8.3 nm. (Fig.10a). Also Table (2) represents the total rate of the particle sizes of the graft co-polymer nanoparticle and the different proportions of these volumes; the results indicate that the molecular size of the graft co-polymer nanoparticle was 74.39 nm. (Fig. 11) represent the distribution of the different proportions of particle sizes of the graft co-polymer nanoparticle.[18, 27]

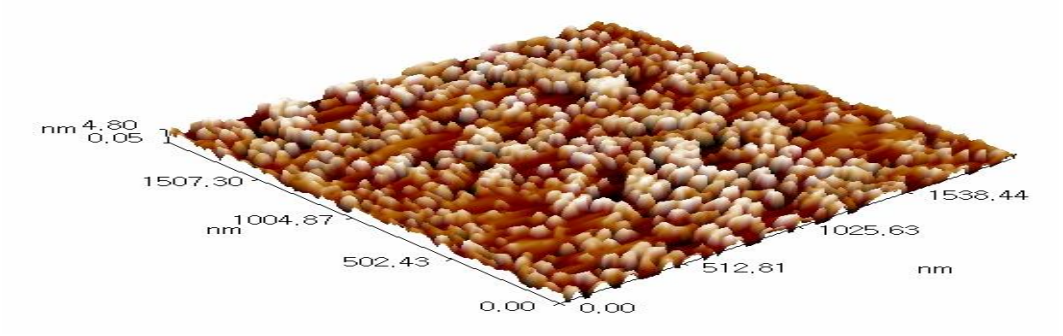

Figure (8a): Image of Atomic Force Microscope for linear co-polymer shows 3D Image.

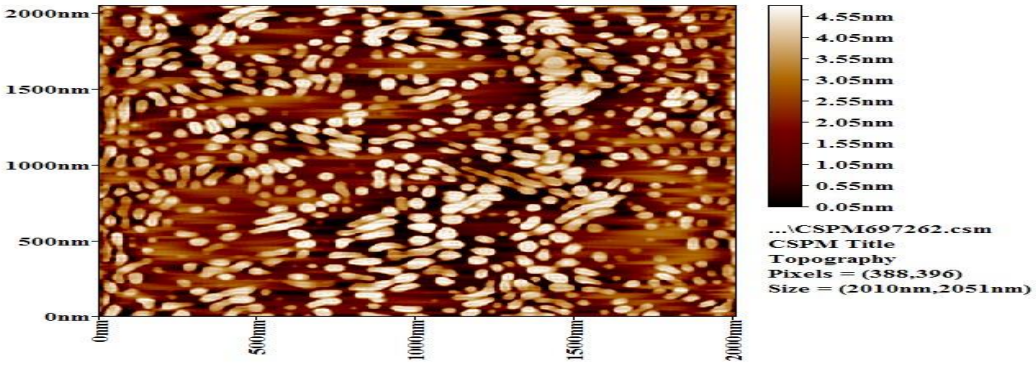

Figure (8 b): Image of Atomic Force Microscope for linear co-polymer shows 2D Image.

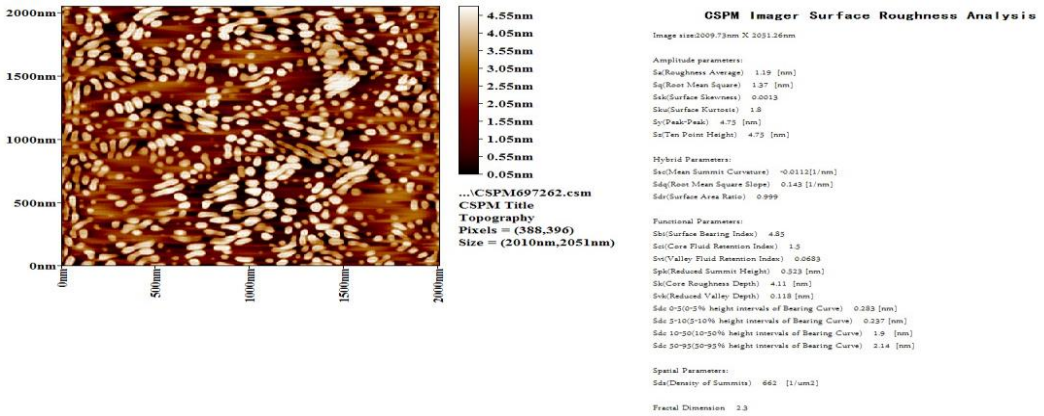

Figure (8 c): Image of Atomic Force Microscope for linear co-polymer shows 2D Image and showing all details of particles

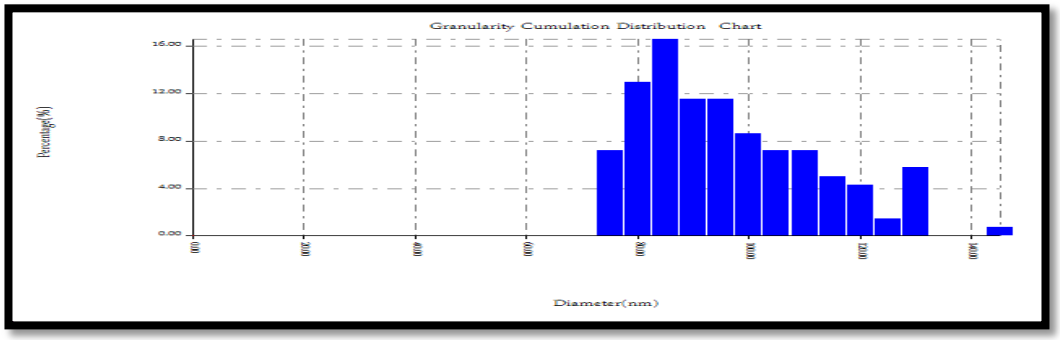

Figure (9): Distribution of the different proportions of particle sizes of the linear co-polymer nanoparticle.

Table (1): The total rate of the particle sizes of the linear co-polymer nanoparticle and the different proportions of these volumes

Sample:1	**Code:** Sample Code
Line No.: lineno	**Grain No.:**139
Instrument: CSPM	**Date:**2018-04-23
Avg. Diameter: 94.09 nm	**<=10% Diameter:75.00 nm**
<=50% Diameter: 90.00 nm	**<=90% Diameter:115.00 nm**

Diameter (nm)<	Volume (%)	Cumulation (%)	Diameter (nm)<	Volume (%)	Cumulation (%)	Diameter (nm)<	Volume (%)	Cumulation (%)
75.00	7.19	7.19	100.00	8.63	68.35	125.00	1.44	93.53
80.00	12.95	20.14	105.00	7.19	75.54	130.00	5.76	99.28
85.00	16.55	36.69	110.00	7.19	82.73	145.00	0.72	100.00
90.00	11.51	48.20	115.00	5.04	87.77			
95.00	11.51	59.71	120.00	4.32	92.09			

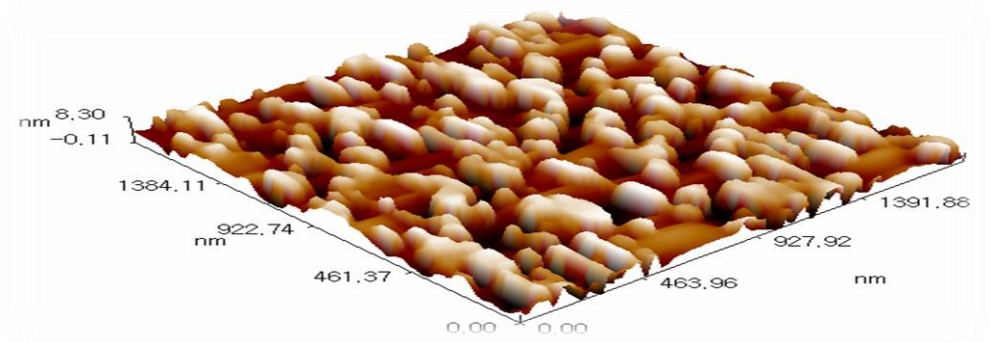

Figure (10 a): Image of Atomic Force Microscope for graft co-polymer shows 3D Image.

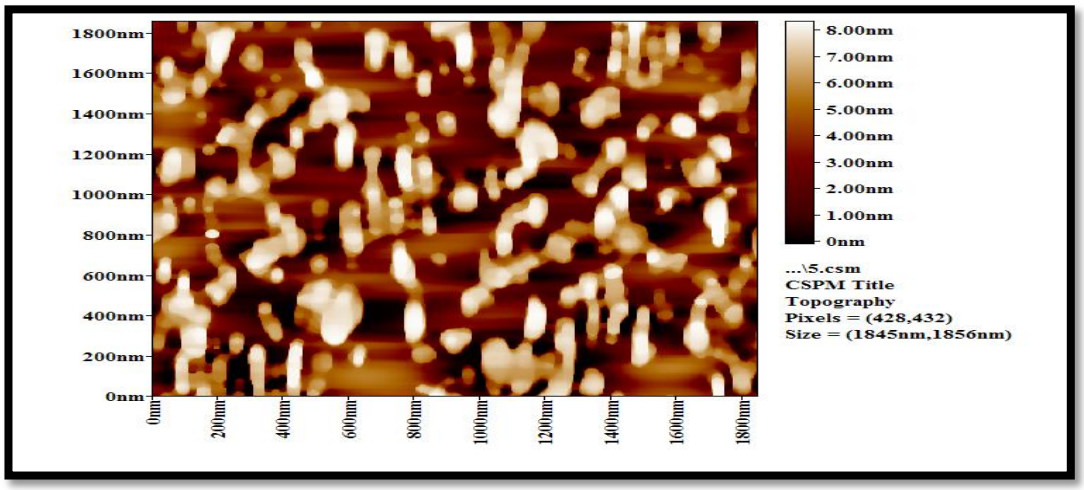

Figure (10 b): Image of Atomic Force Microscope for graft co-polymer shows 2D Image.

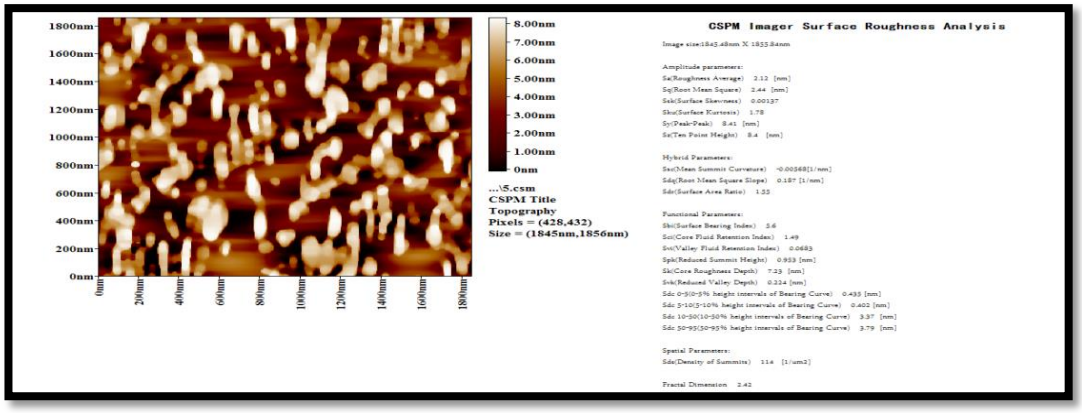

Figure (10 c): Image of Atomic Force Microscope for graft co-polymer shows 2D Image and showing all details of particles.

Table (2): The total rate of the particle sizes of the graft co-polymer nanoparticle and the different proportions of these volumes

Sample:2			**Code:** Sample Code					
Line No.: lineno			**Grain No.:**208					
Instrument: CSPM			**Date:**2019-05-31					
Avg. Diameter:74.39 nm			**<=10% Diameter:0 nm**					
<=50% Diameter:70.00 nm			**<=90% Diameter:95.00 nm**					
Diameter (nm)<	Volume (%)	Cumulation (%)	Diameter (nm)<	Volume (%)	Cumulation (%)	Diameter (nm)<	Volume (%)	Cumulation (%)
55.00	10.58	10.58	85.00	7.69	75.96	115.00	1.44	98.56
60.00	12.98	23.56	90.00	6.73	82.69	120.00	0.48	99.04
65.00	10.10	33.65	95.00	4.81	87.50	125.00	0.48	99.52
70.00	12.50	46.15	100.00	4.33	91.83	140.00	0.48	100.00
75.00	7.21	53.37	105.00	2.88	94.71			
80.00	14.90	68.27	110.00	2.40	97.12			

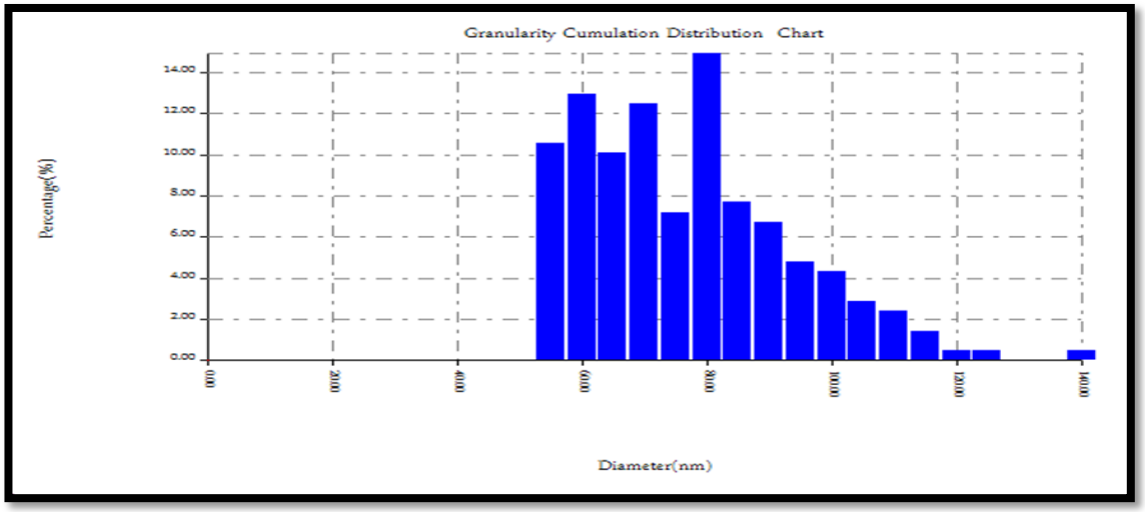

Figure (11): Distribution of the different proportions of particle sizes of the graft co-polymer nanopartical.

3.2. Surface Coverage

The following formula is used to calculate the extent of polymer coverage on the surface of carbon steel.

$\boldsymbol{\theta} = \frac{\boldsymbol{\eta\%}}{\mathbf{100}}$…….. equation (2)

Where, θ : Surface coverage , η% : Inhibition efficiency [19, 20].

3.3. Potentiostatic Polarization Measurement

The potentiostatic polarization technique has been used to study the effect of the presence of deferent moles of inhibitor (0.2 , 0.4 , 0,6 , 0.8) mole , on the corrosion of carbon steel alloy in 1M H_2SO_4 over the range of temperatures (303-323)K , the obtained polarization parameters including corrosion potential (E_{corr}), corrosion current density (I_{corr}), slopes of the linear segments anodic and cathodic (βa), (βc) Tafel slopes, surface coverage (θ) and inhibition efficiency (η%) are shown in Table(3) The results show that raising the concentration enhances the inhibition efficacy at constant temperature, the corrosion current density reduces with the addition of inhibitor to the aggressive media, but increases as temperature rises with a minor shift in the E_{corr} values[28, 29]. Figure (12) shows the polarization curves. In order to better understand how the inhibitor affects the corrosion of carbon steel in 1M H_2SO_4 solution, where Possible measurements of polarization were Made in the presence and absence of Nano-polymer concentrations (0.2, 0.4, 0.6, 0.8) mole at several temperatures (303 - 323) K. 3D illustration for the obtained results is demonstrated in Figure (13).The highest corrosion inhibition efficiency (91.41%) was recorded in the presence of 0.8 mole of inhibitor at 303k in 1M H_2SO_4.

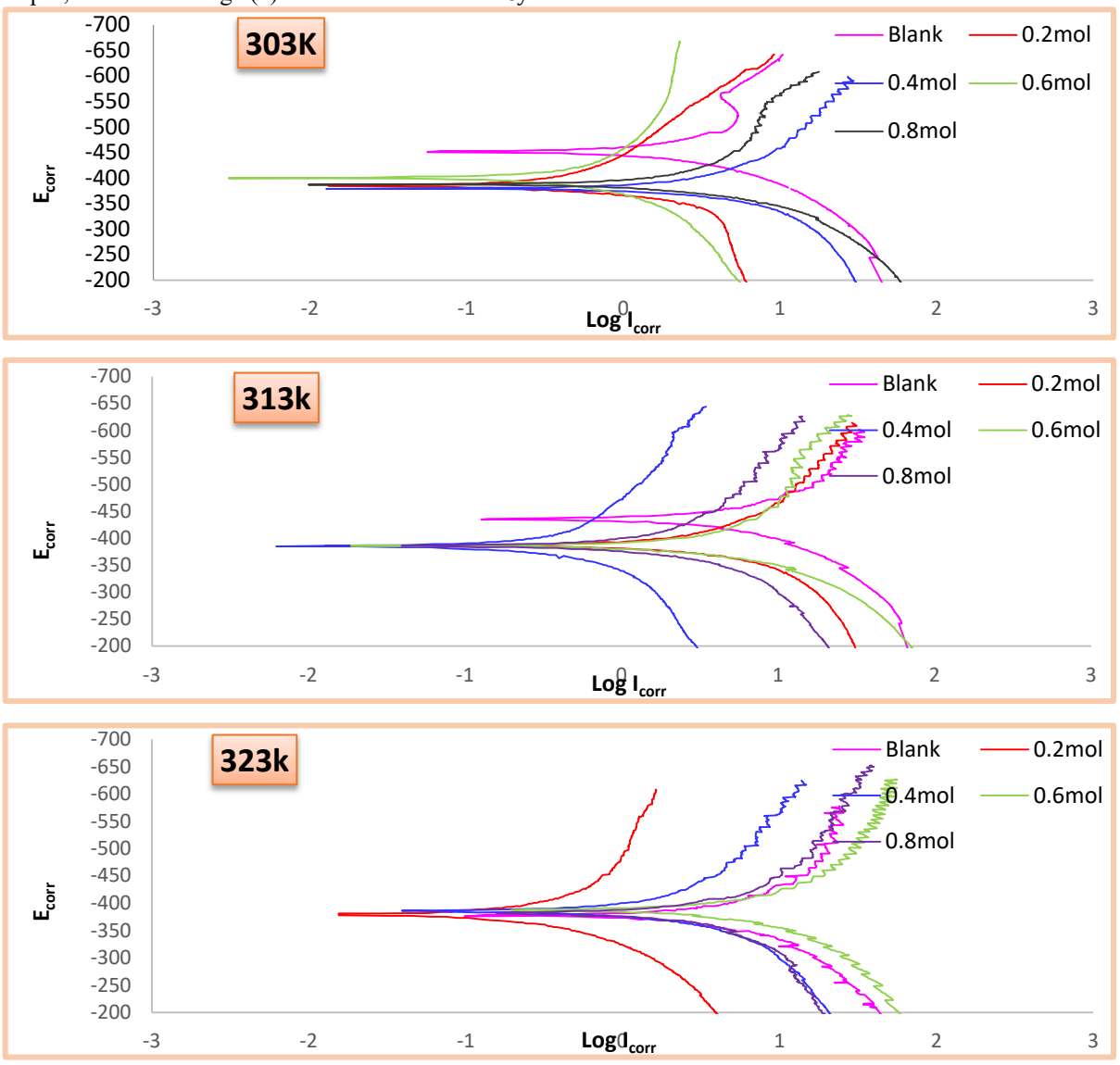

Figure(12): Potentiostatic polarization curves for carbon steel in 1 M H_2SO_4 in the absence and presence of Nano-polymer over temperature range (303–323) K.

Table (3): polarization parameters for the corrosion of carbon steel by different moles of inhibitor in 1M H_2SO_4 at the temperature range (303-323) K

Tem. K	Inhibitor Mol	- E_{cor} (mV)	I_{corr} (µA/cm^2)	β_a (mVdec^{-1})	- β_c (mVdec^{-1})	η%	θ
303	0	452.4	2520	107.6	159.5	0	
313		428.6	2940	77.6	85.4	0	
323		376.1	3220	60.6	190	0	
303	0.2	385.8	821.4	49.6	48.52	67.40476	0.674048
313		386.7	1120.3	67.1	109.8	61.89456	0.618946
323		378.2	1258.6	55.4	73.3	60.91304	0.60913
303	0.4	379.8	701.3	51.4	134.3	72.17063	0.721706
313		385.1	871.5	45.4	61.8	70.35714	0.703571
323		386.3	1025.5	63.3	88.9	68.15217	0.681522
303	0.6	390.0	434.1	44.6	86.3	82.77381	0.827738
313		385.6	580.9	47.2	86.6	80.2415	0.802415
323		387.5	732.5	63	88.3	77.25155	0.772516
303	0.8	387.3	216.4	46.0	82.8	91.4127	0.914127
313		386.0	289.4	52.3	74.1	90.15646	0.901565
323		382.8	352.3	62.3	121.4	89.05901	0.89059

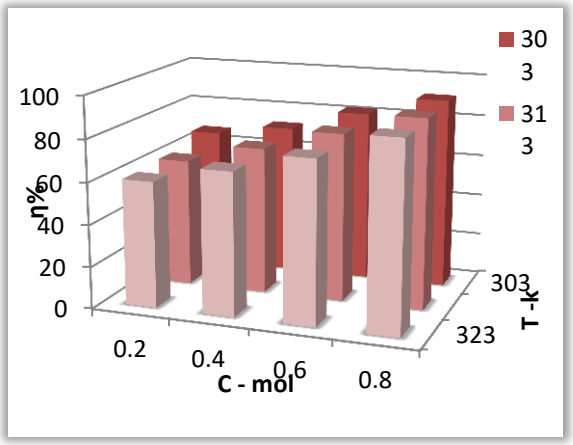

Figure (13): 3D illustration for the variation of the inhibition efficiency at different inhibitor moles in 1 M H_2SO_4 over the temperature range 303–323 K

.

3.4. Adsorption Isotherms

In our work we studied the adsorption isotherms for the Nano- polymer on the carbon steel alloy to know the nature of interaction between the metal surface and the inhibitor molecules nano polymer. The experimental outcomes from the potentiostatic polarization studies are used to test several adsorption isotherms, and the best fitting was found obey Langmuir isotherms model. The adsorption constants (K_{ads}) were calculated according to Langmuir equation (3),

Figure (14) shows the Langmuir relationship for adsorption of Nano-polymer inhibitor in 1 M H_2SO_4 adsorption while values more negative than -40 kJmol^{-1} involved charge sharing or transfer from the acid over the temperature range 303–323 K. equation (4) is used to calculate the Gibbs free energy of the adsorption process (ΔG_{ads}). By equation (5) we can calculate the reaction enthalpy ΔHads from the relationship between logarithm of K_{ads} values were plotted versus 1/T Figure (15) [20, 30, 31].

$$\frac{Cinh}{\theta} = \frac{1}{Kads} + Cinh \ldots\ldots\ldots (3)$$

ΔG_{ads} = - RT ln (55.5 K_{ads}) ……(4)

$$\log K_{ads} = \left(-\frac{\Delta H_{ads}}{2.303\ RT}\right) + Constant \ldots\ldots\ldots\ldots (5)$$

Where (***Cinh)*** is concentration of the inhibitor, (**θ)** is the surface coverage, (**T)** is the absolute temperature and (**R)** is the universal gas constant. The numerical value of 55.5 represents the molar concentration of water in acid solution.

Table (4) shows the adsorption parameters K_{ads}, ΔG_{ads} and ΔH_{ads} their values gives an illustration about the nature of adsorption process and the ability of the nano-polymer to get adsorbed onto the metal surface. The values of Kads were positive in all cases, indicating a favorable adsorption.[32] The higher Kads values refer to high ability for adsorption and the lower the temperature.

The values of ΔG_{ads} were negative; this indicates that the reaction was spontaneous, feasible and high stability of the adsorbed layer of nano-polymer on the metal surface. [33] The calculated value of the ΔG_{ads} that was lower than -20 KJmol^{-1} indicates that the adsorption process is probably by physical adsorption. The negative values of ΔG_{ads} up to -20 kJ mol^{-1} are compatible with electrostatic interactions between the charged metal which signifies physical

inhibitor molecules to the metal surface to form coordinate type of bond which signifies chemical

adsorption.[34-36] The negative ΔH_{ads} values refer to the exothermic nature of the adsorption process[37]. The irregularity of the adsorbed layers on the metal's superficies is indicated by positive ΔS_{ads} values.[29, 38]

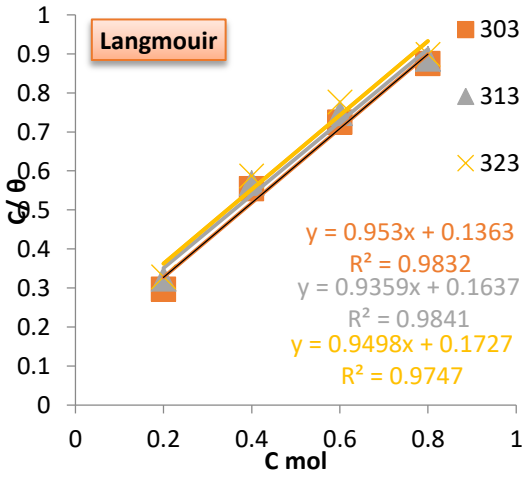

Figure (14): Langmuir relationship for adsorption of Nano-polymer in 1 M H2SO4 acid over temperature range 303–323 K.

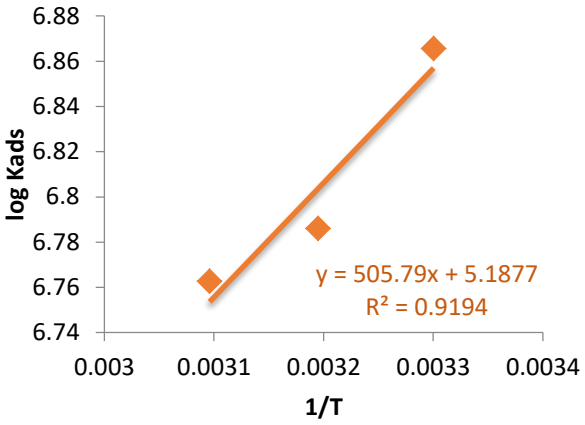

Figure (15): Log *K*ads *versus* 1/*T* for carbon steel with and without Nano-polymer in 1 M sulfuric acid solution over temperature range 303–323 K.

Table (4): The thermodynamic function of the adsorption process for the nano-polymer inhibitor

Medium (M)	Temp. (K)	K_{ads} (mol^{-1})	ΔG_{ads} ($KJ.mol^{-1}$)	ΔS_{ads} ($KJ.mol^{-1}.K^{-1}$)	ΔH_{ads} ($KJ.mol^{-1}$)
1M	323	5790388	-52.6023	0.132873	-9.68443
	313	6108735	-51.113	0.13236	
	303	7336757	-49.9415	0.132861	

3.5. Kinetics of Corrosion

To learn more about the electrochemical behavior of the investigated carbon steel alloy in acidic medium in the absence and presence of Nano-polymer , (The Arrhenius relationship) , Eq. (6)[39], was used to calculate the effect of temperature on corrosion rate. enthalpy (ΔH*), entropy of activation (ΔS*) and Gibbs free energy (ΔG*) were calculated via the equations below" (7,8), where $\mathbf{i_{corr}}$: corrosion current density, **A**: Arrhenius constant, $\mathbf{E_a}$: activation energy, **R**: the gas constant, T: the temperature of the solutions, h: is the blank constant, **N**: is the Avogadro number.[40]

$$\log I_{corr} = \log A - \frac{E_a}{2.303\,RT} \quad \text{.....(6)}$$

$$i_{corr} = \frac{RT}{Nh} e^{\frac{\Delta S*}{R}} e^{-\frac{\Delta H*}{RT}} \quad \text{.....(7)}$$

$$\Delta G^* = \Delta H^* - T\,\Delta S^* \quad \text{.....(8)}$$

Figure (16) show the diagram between (Log i_{corr}) versus (1 / T) for carbon steel alloy corrosion in 1M of H_2SO_4 in the absence and the existence of diversified concentrations of Nano-polymer where the activation energy (E_a) was extracted from the slope of the drawn relationship. Table (5) shows values E_a , ΔH*, ΔS*, ΔG*.The positive values of activation enthalpy (ΔH*) indicate that the reaction is endothermic. Positive Gibbs free energy (ΔG*) values indicate the creation of the spontaneously activated compound, The study shows that the increase in the concentration of the inhibitor increases the activation energy (E_a) and thus the energy barrier for the inhibition reaction increases. The negative values of (ΔS*) in the presence of inhibitors denote the increase in the regularity of the system.[41-45]

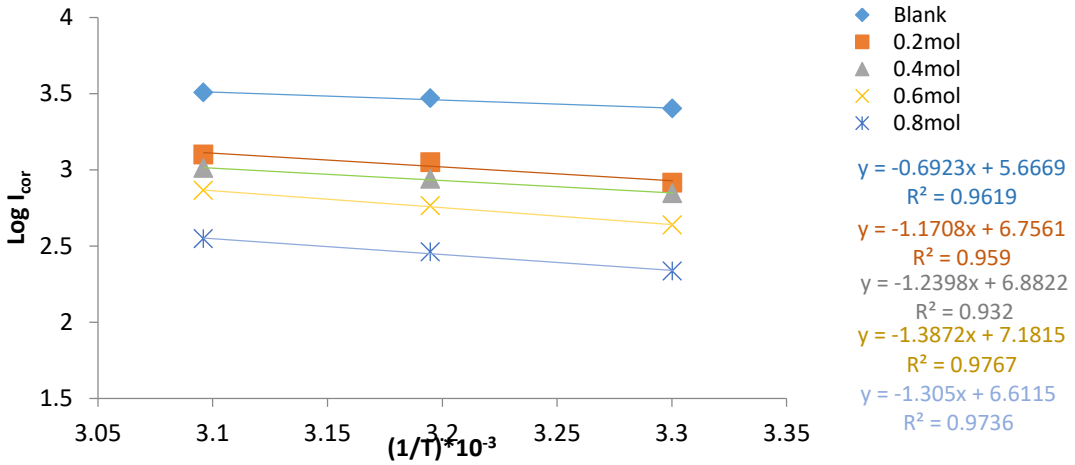

Figure (16): Arrhenius plot of the carbon steel 1M H_2SO_4 at Nano-polymer concentrations at the temperature range 303-323K.

Table (5): ΔH*, ΔS*, ΔG* ,E_a values for the corrosion of carbon steel in the presence and absence several of Nano-polymer concentration. at temperature rang (303-323)K

Inh-mol	ΔH* (KJ.mol^{-1})	E_a (KJ.mol^{-1})	-ΔS* (KJ.mol^{-1}.K^{-1})	ΔG*(KJ.mol^{-1})		
				303 k	313 k	323 k
0	10.69750824	13.2556	0.145024785	54.6400182	56.09026605	57.54051391
0.2	19.8613304	22.4175	0.124171633	57.4853352	58.72705153	59.96876786
0.4	21.18248319	23.7386	0.121755264	58.07432809	59.29188073	60.50943337
0.6	24.00477193	26.5609	0.116024524	59.16020272	60.32044796	61.4806932
0.8	22.43087685	24.987	0.126938395	60.89321055	62.1625945	63.43197845

3.6. Thermodynamic of Corrosion process

The Gibbs free energy for corrosion of carbon steel in 1M H_2SO_4 medium at several temperatures (303-323)K. was calculated using the equation(9). [46]

$$\Delta G = - nFE_{corr} \quad \text{……..(9)}$$

n: The number of electrons flowing from the anodic, **F**: Faradays constant **, Ecorr**: potential cell . The change in enthalpy (ΔH) for the corrosion process is calculated by using the (Gibbs-Helmoholtz) equation (10) by the slope of the linear relationship between (ΔG / T) and (1 / T) as shown in Figure(17).The change in entropy (ΔS) is calculated from the values of (ΔG), (ΔH) according to the following equation(11).[29, 47-51]

$$\Delta G/T = \Delta H/T + cons \quad \text{……(10)}$$

$$\Delta G = \Delta H - T\Delta S \quad \text{……(11)}$$

The thermodynamic amounts ΔG, ΔH and ΔS for carbon steel in 1M H_2SO_4 at several temperatures (303-323) K are presented in Table(6)

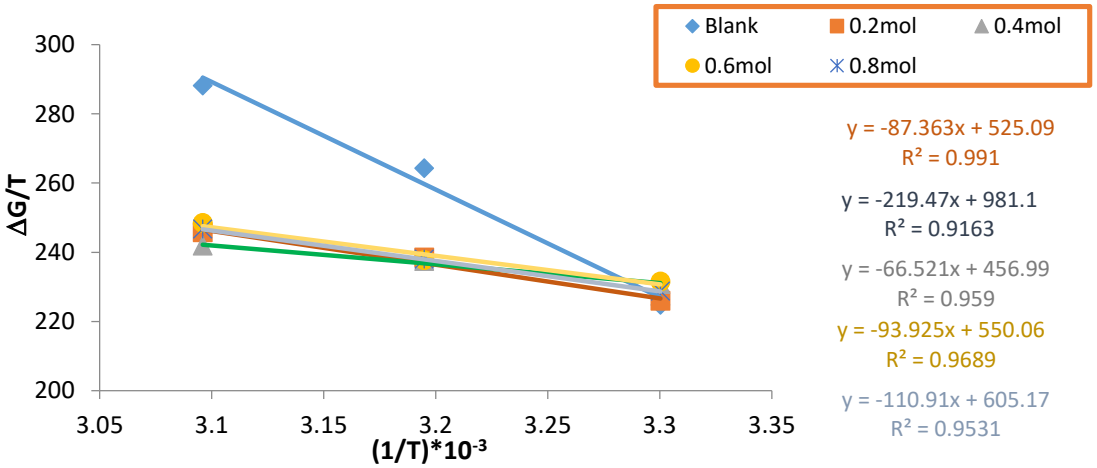

Figure(17): Relationship. Between ΔG/T versus 1/T for inhibition Nano-polymer in 1M H_2SO_4 at the temperature range 303-323K.

Table (6): shows the thermodynamic quantities ΔG, ΔH and ΔS for the carbon steel in the presence and absence different inhibitor concentration at temperature rang (303-323)K

Tem. K	Inhibitor Mol	ΔG (KJ.mol^{-1})	ΔS (KJ.mol^{-1})	ΔH (KJ.mol^{-1})
303	0	87.29992658	-1012.442002	-219.47
313		82.70722488	-965.4224437	
323		72.57626523	-904.1680038	
303	0.2	74.44808063	-534.0299691	-87.363
313		74.62175422	-517.5231764	
323		72.98150361	-496.4226118	
303	0.4	73.29025667	-461.4232893	-66.521
313		74.31300117	-449.9488855	
323		74.54456596	-436.7354983	
303	0.6	75.2585574	-558.3615756	-93.925
313		74.4094865	-537.809861	
323		74.77613075	-522.2945224	
303	0.8	74.73753662	-612.6981407	-110.91
313		74.48667476	-592.3216446	
323		73.86916865	-572.0717296	

4. Conclusions

1- In this study we have proven that Poly (Terphthalic acid-co-Glycerol-G-Maleic anhydride) acts as efficient corrosion inhibitor for carbon steel in 1 M H_2SO_4.

2- The electrochemical analysis revealed that the inhibition efficiency increases with increasing the concentration of Poly (Terphthalic acid-co-Glycerol-G-Maleic anhydride) and decreases the temperature. So in this research the highest result of inhibition efficiency is 91.41% at 0.8 mol of Nano-polymer and at 303 K.

3- The adsorption of Poly (Terphthalic acid-co-Glycerol-G-Maleic anhydride), onto carbon steel surface fits Langmuir adsorption model.

5. References

1. Stark, W.J., et al., *Industrial applications of nanoparticles.* Chemical Society Reviews, 2015. **44**(16): p. 5793-5805.

2. Kim, B.H., et al., *Synthesis, characterization, and application of ultrasmall nanoparticles.* Chemistry of Materials, 2014. **26**(1): p. 59-71.

3. Dong, F., et al., *Nanomaterials for environmental applications*. 2014, Hindawi.

4. Salata, O.V., *Applications of nanoparticles in biology and medicine.* Journal of nanobiotechnology, 2004. **2**(1): p. 1-6.

5. Sabir, S., M. Arshad, and S.K. Chaudhari, *Zinc oxide nanoparticles for revolutionizing agriculture: synthesis and applications.* The Scientific World Journal, 2014. **2014**.

6. Sing, T., et al., *Corrigendum: Application of nanotechnology in food science: Perception and overview*. Frontiers in Microbiology, 2017. **8**: p. 2517.

7. Singh, T., et al., *Application of nanotechnology in food science: perception and overview.* Frontiers in microbiology, 2017. **8**: p. 1501.

8. Rodrigues, S.M., et al., *Nanotechnology for sustainable food production: promising opportunities and scientific challenges.* Environmental Science: Nano, 2017. **4**(4): p. 767-781.

9. King, T., M.J. Osmond-McLeod, and L.L. Duffy, *Nanotechnology in the food sector and potential applications for the poultry industry.* Trends in food science & technology, 2018. **72**: p. 62-73.

10. Guo, D., G. Xie, and J. Luo, *Mechanical properties of nanoparticles: basics and applications.* Journal of physics D: applied physics, 2013. **47**(1): p. 013001.

11. Kumbhakar, P., S.S. Ray, and A.L. Stepanov, *Optical properties of nanoparticles and nanocomposites*. 2014, Hindawi.

12. Hameed, R.A., A.-A.H. Abu-Nawwas, and H. Shehata, *Nano-composite as corrosion inhibitors for steel alloys in different corrosive media.* Advances in Applied Science Research, 2013. **4**(3): p. 126-129.

13. Khodair, Z.T., A.A. Khadom, and H.A. Jasim, *Corrosion protection of mild steel in different aqueous media via epoxy/nanomaterial coating: preparation, characterization and mathematical views.* Journal of Materials Research and Technology, 2019. **8**(1): p. 424-435.

14.Umoren, S. and M. Solomon, *Recent developments on the use of polymers as corrosion inhibitors-a review.* The Open Materials Science Journal, 2014. **8**(1).
15. Jain, P., B. Patidar, and J. Bhawsar, *Potential of nanoparticles as a corrosion inhibitor: a review.* Journal of Bio-and Tribo-Corrosion, 2020. **6**(2): p. 1-12.
16. Valença, D.P., et al., *Study of the efficiency of polypyrrole/ZnO nanocomposites as additives in anticorrosion coatings.* Materials Research, 2015. **18**: p. 273-278.
17.Fotovvati, B., N. Namdari, and A. Dehghanghadikolaei, *On coating techniques for surface protection: A review.* Journal of Manufacturing and Materials processing, 2019. **3**(1): p. 28.
18. Voigtländer, B., *Atomic Force Microscopy*. 2019: Springer International Publishing.
19. Sanumi, O.J., *The Study of Corrosion Inhibition of Polyethylene Glycol-Tyrosine Composite on Mild Steel in 1M HCl*. 2019, University of Johannesburg (South Africa).
20. Abdel-Goad, M., N. Mahmoud, and B. Saad, *The Analysis of Adsorption Phenomenon for Nano silica with Some Radionuclides Released in The Primary Coolant of PWR.* Egyptian Journal of Chemistry, 2020. **63**(5): p. 1655-1667.
21. Rathish, R.J., et al., *Corrosion resistance of nanoparticle-incorporated nano coatings.* European Chemical Bulletin, 2013. **2**(12): p. 965-970.
22. Ates, M., *A review on conducting polymer coatings for corrosion protection.* Journal of adhesion science and Technology, 2016. **30**(14): p. 1510-1536.
23. Benmahammed, I., et al., *Heterocyclic Schiff bases as corrosion inhibitors for carbon steel in 1 M HCl solution: hydrodynamic and synergetic effect.* Journal of Dispersion Science and Technology, 2020. **41**(7): p. 1002-1021.
24. Huffman, R.E., et al., *Absorption Coefficients of Carbon Monoxide in the 1006-600-A Wavelength Region*. 1964: Air Force Cambridge Research Laboratories, Office of Aerospace Research, United States Air Force.
25. Pavia, D.L., et al., *Introduction to Spectroscopy*. 2014: Cengage Learning.
26.Choudhary, M.I., *Applications of NMR Spectroscopy: Volume 9*. 2021: Bentham Science Publishers.
27. Takeyasu, K., *Atomic Force Microscopy in Nanobiology*. 2016: Jenny Stanford Publishing.
28. Satapathy, A., et al., *Corrosion inhibition by Justicia gendarussa plant extract in hydrochloric acid solution.* Corrosion science, 2009. **51**(12): p. 2848-2856.
29. Salman, H.E., A.A. Balakit, and L.B. Jasim, *Azoisonicotinohydrazide derivative as carbon steel corrosion inhibitor in 1 M H2SO4: potentiostatic, adsorption isotherm and surface studies.* Int. J. Corros. Scale Inhib, 2019. **8**(3): p. 539-548.
30. Ghaedi, M., *Adsorption: Fundamental Processes and Applications*. 2021: Elsevier Science.
31. Umoren, S.A., I.B. Obot, and Z.M. Gasem, *Adsorption and corrosion inhibition characteristics of strawberry fruit extract at steel/acids interfaces: experimental and theoretical approaches.* Ionics, 2015. **21**(4): p. 1171-1186.
32. Yaro, A.S. and D.A. Abdulaaima, *Phenyl thiourea as corrosion inhibitor for mild steel in strong hydrochloric acid.* Iraqi Journal of Chemical and Petroleum Engineering, 2012. **13**(2): p. 1-9.
33. Verma, C., et al., *L-Proline-promoted synthesis of 2-amino-4-arylquinoline-3-carbonitriles as sustainable corrosion inhibitors for mild steel in 1 M HCl: experimental and computational studies.* RSC advances, 2015. **5**(104): p. 85417-85430.
34. Umoren, S., et al., *Gum arabic as a potential corrosion inhibitor for aluminium in alkaline medium and its adsorption characteristics.* Anti-corrosion methods and materials, 2006.
35. Sherif, E.-S.M., *Electrochemical investigations on the corrosion inhibition of aluminum by 3-amino-1, 2, 4-triazole-5-thiol in naturally aerated stagnant seawater.* Journal of Industrial and Engineering Chemistry, 2013. **19**(6): p. 1884-1889.
36. Salman, H.E., A.A. Balakit, and M.A.A.H. Allah. *Study of the corrosion inhibitive effect and adsorption process of two azo-aldehydes on carbon steel in 1 M H2SO4*. in *IOP Conference Series: Materials Science and Engineering*. 2019. IOP Publishing.
37. Verma, C., M. Quraishi, and A. Singh, *2-Amino-5-nitro-4, 6-diarylcyclohex-1-ene-1, 3, 3-tricarbonitriles as new and effective corrosion inhibitors for mild steel in 1 M HCl: Experimental and theoretical studies.* Journal of Molecular Liquids, 2015. **212**: p. 804-812.
38. Hassan, S. and A. Hadi, *Sudan III as corrosion ınhıbıtor for carbon steel St37− 2 in H2SO4 solutıons.* International Journal of Recent Scientific Research, 2015. **6**: p. 5445-5453.
39. ÖZKIR, D., et al., *Thermodynamic study and electrochemical investigation of calcein as corrosion Inhibitor for mild steel in hydrochloric acid Solution.* Journal of the Chilean Chemical Society, 2013. **58**(4): p. 2158-2167.
40. Sliem, M.H., et al., *AEO7 surfactant as an eco-friendly corrosion inhibitor for carbon steel in HCl solution.* Scientific reports, 2019. **9**(1): p. 1-16.
41. Yaro, A.S. and A.A. Khadom, *Evaluation of the performance of some chemical inhibitors on*

corrosion inhibition of copper in acid media. Journal of Engineering, 2008. **2**(14): p. 2350-2362.
42. Hamani, H., et al., *Corrosion inhibition efficiency and adsorption behavior of azomethine compounds at mild steel/hydrochloric acid interface.* Measurement, 2016. **94**: p. 837-846.
43. Da Rocha, J.C., J.A.d.C.P. Gomes, and E. D'Elia, *Corrosion inhibition of carbon steel in hydrochloric acid solution by fruit peel aqueous extracts.* Corrosion Science, 2010. **52**(7): p. 2341-2348.
44. Heakal, F.E.-T., A. Fouda, and S. Zahran, *Environmentally safe protection of carbon steel corrosion in sulfuric acid by thiouracil compounds.* Int. J. Electrochem. Sci, 2015. **10**: p. 1595-1615.
45. El Ouali, I., et al., *Thermodynamic characterisation of steel corrosion in HCl in the presence of 2-phenylthieno (3, 2-b) quinoxaline.* J. Mater. Environ. Sci, 2010. **1**(1): p. 1-8.
46. Hamani, H., et al., *1-(4-Nitrophenylo-imino)-1-(phenylhydrazono)-propan-2-one as corrosion inhibitor for mild steel in 1 M HCl solution: weight loss, electrochemical, thermodynamic and quantum chemical studies.* Journal of Electroanalytical Chemistry, 2017. **801**: p. 425-438.
47. Bedair, M., et al., *Synthesis, electrochemical and quantum chemical studies of some prepared surfactants based on azodye and Schiff base as corrosion inhibitors for steel in acid medium.* Corrosion Science, 2017. **128**: p. 54-72.
48. Singh, D.K., et al., *Non-toxic Schiff bases as efficient corrosion inhibitors for mild steel in 1 M HCl: Electrochemical, AFM, FE-SEM and theoretical studies.* Journal of Molecular Liquids, 2018. **250**: p. 88-99.
49.Albo Hay Allah, M.A., et al., *New heterocyclic compound as carbon steel corrosion inhibitor in 1 M H2SO4, high efficiency at low concentration: Experimental and theoretical studies.* Journal of Adhesion Science and Technology, 2022: p. 1-23.
50. Emad Salaam Abood, Amer Mousa Jouda, and Muthana Saleh Mashkoor**,** *Zinc Metal at a New ZnO Nanoparticle Modified Carbon Paste Electrode: A Cyclic Voltammetric Study.* Nano Biomed. Eng., 2018, **10**(2): 149-155.
51. Abood, Emad Salaam, Ahmed Salim Abed, and Zahara Njah Salman. *"New Fe2O3 Nanoparticles Modified Carbon Paste Electrode: A Cyclic Voltammetric Study."* Egyptian Journal of Chemistry **64**.12 (2021): 7409-7415.